AGU PUBLICATIONS

JGR

Journal of Geophysical Research: Biogeosciences

RESEARCH ARTICLE

10.1002/2016JG003695

Both authors M. J. Kurz and J. D. Drummond contributed equally to this work.

Key Points:
- Ecosystem respiration is positively correlated with water depth, discharge, and vegetation coverage
- In-stream vegetation beds are significant sites of metabolically active transient storage
- Declining stream flows may negatively impact aquatic vegetation and ecosystem function in lowland rivers

Supporting Information:
- Supporting Information S1

Correspondence to:
M. J. Kurz,
marie.kurz@drexel.edu

Citation:
Kurz, M. J., et al. (2017), Impacts of water level on metabolism and transient storage in vegetated lowland rivers: Insights from a mesocosm study, *J. Geophys. Res. Biogeosci.*, *122*, 628–644, doi:10.1002/2016JG003695.

Received 31 OCT 2016
Accepted 27 FEB 2017
Accepted article online 2 MAR 2017
Published online 20 MAR 2017

©2017. American Geophysical Union. All Rights Reserved.

Impacts of water level on metabolism and transient storage in vegetated lowland rivers: Insights from a mesocosm study

Marie J. Kurz[1,2], Jennifer D. Drummond[3], Eugènia Martí[3], Jay P. Zarnetske[4], Joseph Lee-Cullin[4], Megan J. Klaar[5,6], Silvia Folegot[5], Toralf Keller[1], Adam S. Ward[7], Jan H. Fleckenstein[1], Thibault Datry[8], David M. Hannah[5], and Stefan Krause[5]

[1]Department of Hydrogeology, Helmholtz Centre for Environmental Research-UFZ, Leipzig, Germany, [2]Patrick Center for Environmental Research, The Academy of Natural Sciences of Drexel University, Philadelphia, Pennsylvania, USA, [3]Integrative Freshwater Ecology Group, Centre for Advanced Studies of Blanes (CEAB-CSIC), Blanes, Spain, [4]Department of Earth and Environmental Sciences, Michigan State University, East Lansing, Michigan, USA, [5]School of Geography, Earth and Environmental Sciences, University of Birmingham, Birmingham, UK, [6]School of Geography, University of Leeds, Leeds, UK, [7]School of Public and Environmental Affairs, Indiana University, Bloomington, Bloomington, Indiana, USA, [8]IRSTEA, UR-MALY, Centre de Lyon-Villeurbanne, Villeurbanne, France

Abstract Transient storage zones for water represent potential hot spots for metabolic activity in streams. In lowland rivers, the high abundance of submerged vegetation can increase water transient storage, bioreactive surface areas, and, ultimately, in-stream metabolic activity. Changes in flow resulting from climatic and anthropogenic factors that influence the presence of aquatic vegetation can also, thereby, impact in-stream metabolism and nutrient cycling. We investigated the effects of water column depth on aquatic vegetation cover and its implications on water transient storage and associated metabolic activity in stream mesocosms ($n = 8$) that represent typical conditions of lowland streams. Continuous injections of metabolically reactive (resazurin-resorufin) tracers were conducted and used to quantify hydraulic transport and whole-mesocosm aerobic respiration. Acetate, a labile carbon source, was added during a second stage of the tracer injection to investigate metabolic responses. We observed both higher vegetation coverage and resazurin uptake velocity, used as a proxy of mesocosm respiration, with increasing water column depth. The acetate injection had a slight, positive effect on metabolic activity. A hydrodynamic model estimated the water transport and retention characteristics and first-order reactivity for three mesocosms. These results suggest that both the vegetated surface water and sediments contribute to metabolically active transient storage within the mesocosms, with vegetation having a greater influence on ecosystem respiration. Our findings suggest that climate and external factors that affect flow and submerged vegetation of lowland rivers will result in changes in stream respiration dynamics and that submerged vegetation is a particularly important and sensitive location for stream respiration.

1. Introduction

Stream flow, a master variable shaping the structure and functioning of stream ecosystems [*Poff et al.*, 1997], is sensitive to a number of climatic and anthropogenic factors including climate change, droughts, and altered flow regimes due to abstraction, flood mitigation policies, and reservoir releases [*Wright and Berrie*, 1987; *Bunn and Arthington*, 2002; *Westwood et al.*, 2006]. Climate change is predicted to change the hydrological behavior of streams by altering both the amplitude and the seasonality of flow [*Laizé et al.*, 2014; *Watts et al.*, 2015]. Decreases in flow associated with drought, for example, can result in decreases in stream surface connectivity, increases in water temperature, major shifts in nutrient concentrations and particulate matter, and subsequent profound effects on macroinvertebrates, algae, and microbial communities [*Stanley et al.*, 1997; *Dahm et al.*, 2003; *Lake*, 2003; *James et al.*, 2008; *von Schiller et al.*, 2011, 2015; *Stubbington et al.*, 2015]. These natural low flow effects may be exacerbated when coupled with human flow-altering activities, such as water abstraction or diversion [*Wilby et al.*, 2010; *Arroita et al.*, 2015]. Still largely unknown is the response of stream ecosystem functions, such as metabolism and nutrient cycling, to low flow conditions. Improving our understanding of low flow effects on river ecosystems is critical to predicting the response of aquatic ecosystems to reduced flow resulting from climate change and increased human pressures on water resources. Lowland rivers, and their characteristic beds of aquatic vegetation, may be particularly sensitive to these

effects [*Flynn et al*., 2002; *Franklin et al*., 2008]. The central objective of this work is, therefore, to assess the functional response of vegetation-rich lowland stream ecosystems to reduced stream flows.

Important interactions can occur between flow and aquatic vegetation [*Koch*, 2001; *Franklin et al*., 2008; *Gurnell*, 2014], which can, in turn, have implications for the functioning of the stream ecosystem [*Clarke*, 2002]. Flow regime, including variability in water depth and velocity, has been cited as the most significant environmental parameter affecting the presence, abundance, and diversity of aquatic vegetation [*French and Chambers*, 1997; *Wilby et al*., 1998; *Westwood et al*., 2006; *Franklin et al*., 2008; *Bornette and Puijalon*, 2010]. The importance of flow has led the European Water Framework Directive to use hydrology (including defining and maintaining optimal flow and water depths) as a supporting element in stream ecosystem health and status [*Acreman and Ferguson*, 2010; *Acreman et al*., 2014]. The mechanisms by which flow affects aquatic vegetation and the resulting correlations between flow and vegetation can differ between high and low flow. For example, physical and mechanical stress at high flow velocities can restrict vegetation abundance and, consequently, metabolism and nutrient retention [*Koch*, 2001; *Franklin et al*., 2008], while vegetation growth rates and metabolic functioning can be indirectly limited at low flow by thicker diffusive boundary layers and associated flow-mediated reductions in carbon availability and carbon mass transfer [*Koch*, 2001; *Dahm et al*., 2003].

Aquatic vegetation can influence stream ecosystem function both directly and indirectly by influencing hydrological retention, streambed morphology, geochemistry, and ecological community structure. Localized hydraulic effects promote fine sediment accumulation around aquatic vegetation, which in turn can enhance in-stream biogeochemical cycling [*Sand-Jensen*, 1998; *Kleeberg et al*., 2010; *Drummond et al*., 2014]. Autotrophic production by the vegetation itself and by associated epiphytic communities also influences nutrient cycling and diel variations in dissolved oxygen concentration [*Wilcock et al*., 1999; *Clarke*, 2002; *Riis et al*., 2012; *O'Brien et al*., 2013; *Peipoch et al*., 2014; *Levi et al*., 2015]. Aquatic vegetation also serves as an important refugia and habitat zone [*Phillips*, 2003; *Warfe and Barmuta*, 2006], by enhancing stream hydraulic heterogeneity and altering sedimentation patterns, shading, and thermal regimes [*Sand-Jensen*, 1998; *Wilcock et al*., 1999; *Clarke*, 2002; *O'Brien et al*., 2013; *Rajwa-Kuligiewicz et al*., 2015].

Aquatic vegetation can also play a key role in controlling water and solute transport within transient storage (TS) zones within lowland streams, although the metabolic activity associated with this storage is unknown. Water level and stream flow influence the interaction of the overlying water with slower-moving waters in TS zones; these slower-moving waters are known to be important biogeochemical hot spots [*Thomas et al*., 2003; *Battin et al*., 2008; *Alexander et al*., 2009; *Boano et al*., 2014]. Slower stream flow velocities and longer residence times within these zones can favor vegetation growth and facilitate interaction between solutes and microbial and/or epiphytic communities, potentially increasing ecosystem functions such as nutrient uptake and metabolism [*Bencala and Walters*, 1983; *Koch*, 2001; *Fellows et al*., 2006]. However, not all TS zones are equally bioreactive [e.g., *Argerich et al*., 2011]. Larger TS zones can be correlated with enhanced biogeochemical cycling [*Valett et al*., 1996; *Mulholland et al*., 2001; *Ensign and Doyle*, 2005] but are not always [*Webster et al*., 2003; *Simon et al*., 2005]. Rather, the time water spends within TS zones has been shown to be a better indicator of the potential for nutrient uptake than the size of the TS zone [*Drummond et al*., 2016]. Previous studies that aimed to characterize metabolically active and inactive zones of TS within streams have used the hydrometabolic "smart" tracer resazurin (Raz) [*Haggerty et al*., 2009; *Argerich et al*., 2011]. Raz, a weakly fluorescent dye, irreversibly transforms to resorufin (Rru), a highly fluorescent dye, under mildly reducing conditions. Raz transformation can, therefore, be used as a proxy for aerobic respiration within streams, assuming that the Raz tracer is exposed to all reactive regions within the stream [*Haggerty et al*., 2008; *González-Pinzón et al*., 2014]. To date, applications of the Raz-Rru tracer system have focused on streams without abundant aquatic vegetation and have considered that the primary location of metabolically active TS is associated with the hyporheic zone and/or benthic biofilms, as opposed to components that generate TS zones in surface water column [*Haggerty et al*., 2009; *Argerich et al*., 2011; *González-Pinzón et al*., 2014]. This may be the case in many upland, forested streams where most of these previous studies were conducted; however, in lowland streams with open canopies, submersed aquatic vegetation can also contribute to water TS and associated bioreactivity.

To improve our understanding on the effect of stream flow variation on ecological functioning of lowland rivers, we investigated the joint effects of changes in water depth and aquatic vegetation cover on water

transient storage and ecosystem metabolic activity, as quantified as ecosystem respiration using the Raz tracer approach. This study was conducted in a series of stream mesocosms that simulated conditions of aquatic vegetation development in lowland streams but varied in hydraulic conditions. Since availability of dissolved organic carbon is expected to change with hydrological changes [*von Schiller et al.*, 2015], we further tested the response of the metabolic activity in these mesocosms to a carbon source (acetate) injection. The use of mesocosms for this study, although a simplified version of in-stream conditions, provided comparable, controlled environmental conditions that limited the confounding effects of transient conditions (e.g., seasonal variation, disturbance, and recovery history) or between-site heterogeneity on our study results. We hypothesized that the overall physical and metabolically active TS would predominantly be a function of aquatic vegetation abundance.

2. Methods

2.1. Experimental Design

We injected a reactive (Raz-Rru system) tracer in eight stream mesocosms that were controlled for different water depth conditions, with the combined Raz + Rru acting as a conservative tracer. All mesocosms contained a fixed sediment volume and a gradient of vegetation coverage. Acetate was injected during a second phase of the tracer experiment to examine whether metabolic activity in the mesocosm was stimulated by this dissolved organic carbon source. The profiles of Raz and Rru tracer concentration along each mesocosm were used to estimate whole-mesocosm transformation rates, the results of which were correlated to mesocosm characteristics. In addition, three of the mesocosms were intensively instrumented to facilitate continuous tracer measurements and diel variation of dissolved oxygen concentrations. Within these three intensively instrumented mesocosms, a hydrodynamic model was used to account for flow dynamics as an independent variable, by providing detailed characterizations of solute transport and retention, and first-order reactivity of Raz to Rru.

2.2. Description of the Mesocosms

The experiment was conducted at the Drought Impacts on Stream Ecosystem Functioning (DRI-STREAM) mesocosm facility at Fobdown Watercress Farm, Vitacress Ltd, New Alresford, Hampshire (51.102083, −1.186870), UK. All mesocosms were constructed to be identical—each was 14.5 m long by 0.5 m wide with a bottom layer of homogeneous coarse gravel arranged into a series of four alternating pools and riffles. At the time of the experiments, the average measured sediment depths ranged from 18 cm in pools to 23 cm at riffles (Figure 1d). The design of the long-term DRI-STREAM project consisted of controlling hydrology in each to maintain differences in water depth among the mesocosms. This was done using a weir at the downstream end of each flume. Water depths were maintained at 7, 10, 25, or 35 cm, as measured in the pools, with average water depths ranging from 3.4 to 31.2 cm (Table 1). All other hydraulic parameters, including discharge and residence time, varied between mesocosms (Table 1). All mesocosms were at hydrologic steady state during the experiment and were fed from a common (chalk aquifer) groundwater source.

The mesocosms were planted with *Ranunculus penicillatus* fragments at 2 m spacing in August 2013, 8 months prior to this experiment, and left to passively recruit a mixture of submerged, emergent, and terrestrial vegetation, per the design of the ongoing DRI-STREAM project. The dominant vegetation type at the time of this experiment was submerged *Ranunculus penicillatus* and, to a lesser extent, emergent *Berula* spp., *Rumex* spp., and *Rorippa* spp., and terrestrial *Epilobium* spp. Spatial vegetation coverage in all mesocosms was estimated from photographic surveys taken during the experiments (Figures 1b–1d and Table 1).

The eight mesocosms included two replicates of each of the four water depth treatments (7, 10, 25, and 35 cm). The mesocosms are identified hereafter by their unique code and the controlled water depth condition measured in pools (e.g., 1–25 = mesocosm #1 and 25 cm water depth) (Figure 1). Sediment depths and water depths in the three intensively studied mesocosms (1–25, 2–10, and 3–07) were surveyed at a spatial resolution of 5 × 39 points (12.5 × 36.25 cm), for a total of 195 survey points per mesocosm. The results of these surveys were used to calculate the total water-saturated volume in the mesocosms (including surface water and saturated sediment), the total sediment volume, the total surface water volume, and the ratio of the sediment volume to the surface water volume. The results of the surveys combined with maps of spatial vegetation coverage were further used to calculate the total and percentage vegetated surface water area,

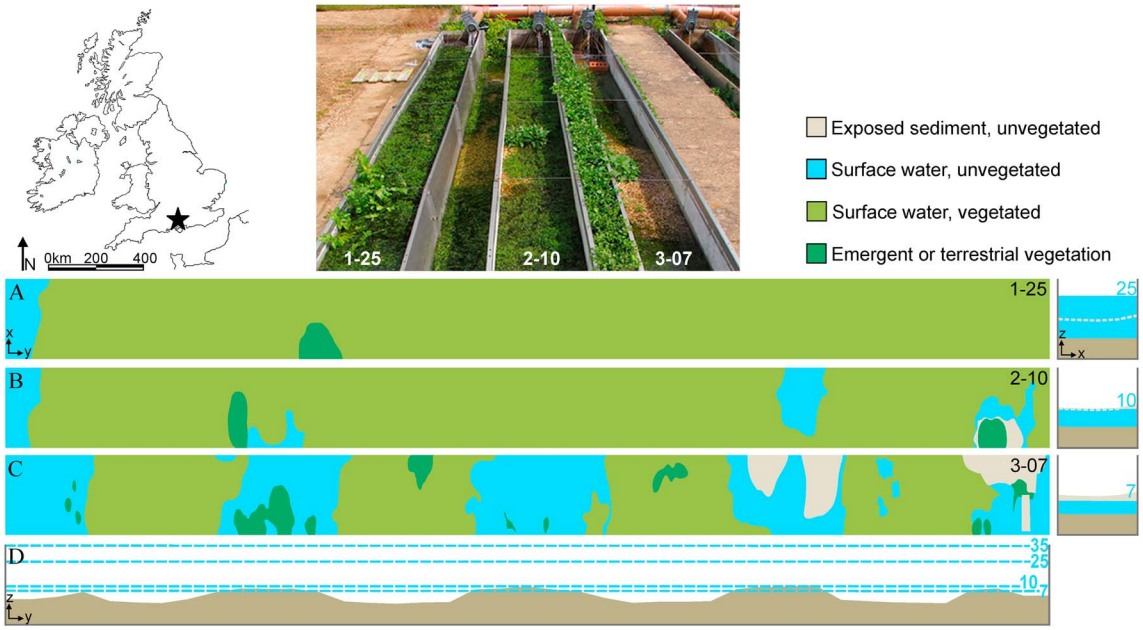

Figure 1. DRI-STREAM mesocosm facility in Hampshire, UK. Maps of vegetation coverage in mesocosms (a) 1-25, (b) 2-10, and (c) 3-07, including, to the right, lateral mesocosm cross sections indicating sediment and water depths. (d) Longitudinal mesocosm cross section showing the average sediment profile, based on mesocosms 1-3, and the four different water depths of mesocosms treatments. Flow is from left to right. Submerged aquatic vegetation dominates in the deeper mesocosms and pool sections of shallowest mesocosms. Submerged aquatic vegetation, when present, filled the entire water column. Mesocosm hydraulic, sediment, and vegetation parameters are summarized in Table 1.

the total and percentage vegetated surface water volume, and the total and percentage unvegetated surface water volume (i.e., open water). The average sediment depth distribution in the three surveyed mesocosms and the known pool water depths for all mesocosms were used to calculate the total and percentage of volume metrics for the remaining five mesocosms that were not intensively characterized.

2.3. Tracer Injection Studies

2.3.1. Raz-Rru System

A constant rate injection of the reactive tracer Raz was conducted from 12:18 to 20:06 on 24 April 2014 (GMT + 1). A 58 L solution of 80.1 g Raz, to target a 100 ppb concentration within the mesocosm, was prepared. The tracer was pumped at a rate of approximately 2 mL s^{-1} into the main mesocosm header tank, to thoroughly

Table 1. Hydraulic, Sediment, and Vegetation Conditions in the Experimental Mesocosms[a]

Mesocosm Number	Average Water Depth (cm)	Discharge ($\times 10^{-4}$ m^3 s^{-1})	Velocity ($\times 10^{-2}$ m s^{-1})	Vegetated Area (%)	Total Volume (m^3)	Vegetated Surface Water Volume (%)	Unvegetated Surface Water Volume (%)	Sediment Volume (%)	Sediment Volume: Surface Water Volume
3-07	3.4	0.375	0.22	56.0	1.53	13.7	3.2	83.1	5.1
4-07[b]	3.8	1.09	0.57	87.3	1.58	16.7	0.8	82.6	4.7
2-10	7.2	4.77	1.37	90.6	1.86	26.1	1.1	72.8	2.7
9-10[b]	6.3	2.68	0.85	87.1	1.76	24.7	1.2	74.2	2.9
1-25	23.4	13.0	1.11	96.7	2.97	55.1	2.2	42.7	0.7
12-25[b]	21.2	27.0	2.54	92.0	2.84	49.7	4.5	45.9	0.8
6-35[b]	31.2	26.3	1.69	93.8	3.57	59.4	4.1	36.5	0.6
10-35[b]	31.2	34.5	2.21	94.1	3.58	59.5	3.9	36.5	0.6

[a]Values reported as a percentage of the total mesocosm area (7.25 m^2) or the total inundated volume (including sediment and surface water, and volume variable based on water depth).
[b]Sediment and vegetated surface water volumes estimated based on the average measured sediment depths in mesocosms 1-25, 2-10, and 3-07 and the known pool water depths.

mix the tracer prior to distribution to all mesocosms. This header tank mixing ensured that an equal tracer concentration entered the inlet of all mesocosms. The injection flow rate from the reservoir was measured regularly (approximately every 15 min) throughout the injection experiment to account for its potential variation. Concentrations of Raz and Rru were measured continuously at the outflow of mesocosms 1–25, 2–10, and 3–07 using calibrated in situ fluorometers (GGUN FL30, Albillia Co., Neuchatel, Switzerland; 10 s frequency). The conservative tracer NaCl was also injected in parallel from a separate reservoir into the header tank. The resulting increase in specific conductivity from background was minimal (a mean increase of 70 $\mu S\,cm^{-1}$) and was only used to confirm plateau conditions were reached at the mesocosms that were not equipped with an in situ fluorometer.

In addition to the continuous tracer measurements at the outlet of the mesocosms, longitudinal tracer profiles of Raz and Rru concentrations were measured during conservative tracer concentration plateau at all eight mesocosms (3-07, 4-07, 2-10, 9-10, 1-25, 12-25, 6-35, and 10-35). During the plateau, one set of nine water samples were collected every 1.45 m along each mesocosm. Water samples were immediately shielded from light and stored at 4°C until they were analyzed for Raz and Rru on site within 6 h of collection using a fourth calibrated GGUN fluorometer. Conductivity was measured in situ at each water sampling location using a handheld conductivity meter (WTW GmbH, Munich, Germany).

2.3.2. Acetate Injection

An additional constant rate injection of sodium acetate trihydrate (hereafter "acetate") was conducted over the last 3 h of the Raz tracer injection. The acetate injection started at 16:50 and ended at 20:06. Acetate is a known labile carbon source that can stimulate aerobic and anaerobic respiration and has been used in similar tracer injection experiments [e.g., *Baker et al.*, 2000; *Zarnetske et al.*, 2011]. An acetate mass of 59.13 g was injected at a rate of 2 $mL\,s^{-1}$ for a target plateau acetate concentration of 1 ppm. Approximately 2 h after the acetate injection started, when the NaCl injection appeared to have reached a plateau, we collected a second set of nine water samples along each of the mesocosms and analyzed them for Raz and Rru. We then compared Raz and Rru longitudinal profiles at plateau before and during the acetate injection to assess any immediate response of metabolism to the acetate injection.

2.4. Daily Rates of Metabolism and Metabolic Activity Estimates

2.4.1. Estimates of Daily Rates of Whole-Mesocosm Metabolism

Dissolved oxygen (DO) concentration and water temperature were measured continuously at the outflows of the three intensively studied mesocosms (1-25, 2-10, and 3-07) at 10 min frequency from 23 April 2014 13:00 to 25 April 2014 14:00 using in situ sensors (miniDOT Logger, PME Inc., Vista CA, USA). These data were used to calculate daily rates of whole-mesocosm ecosystem respiration (ER), gross primary production (GPP), and net primary production (NPP) [*Bott*, 1996]. Reaeration was estimated from the slope of the linear regression between the net DO change rate and the DO saturation deficit between 20:00 and 23:00, averaged over the two nights, following the night time method [*Young and Huryn*, 1996]. Observed changes in reaeration are presumed to be the result of differences between mesocosms, and not to differences in inflow, as the turbulent, open-air mixing by the pump and groundwater source should have ensured fully saturated and temporally constant inflow DO concentrations.

2.4.2. Estimates of Metabolic Activity From Raz-Rru Transformation Rates

Raz-Rru transformation rates were calculated from the longitudinal tracer profiles taken during the plateau before and during the acetate injection. The following analytical solution to the coupled parent-daughter steady state transport and multirate mass transfer was used to describe the transformation rate of Raz to Rru ($k_{t_{ad}}$, h^{-1}) during the injection experiment [*Haggerty*, 2013, equation (24)]:

$$\ln\left({C_{Rru}}/{C_{Raz}} + P\right) = k_{t_{ad}} t_{ad} + \ln\left({C_{Rru,0}}/{C_{Raz,0}} + P\right) \quad (1)$$

where C_{Rru} and C_{Raz} are the concentrations of Rru and Raz (ppb), t_{ad} is the advective travel time (h), $C_{Rru,0}$ and $C_{Raz,0}$ are the concentrations of Rru and Raz at the inlet of the mesocosm during the plateau (ppb), and P is the production-decay ratio P (-). The production-decay ratio P includes effects of irreversible sorption, photodecay, and any other mass losses of Raz and Rru. We assume that within the timescale of the mesocosm experiments Raz decays only to Rru, Rru is stable, and there are no other mass losses; therefore, $P = 1$. The concentration of Rru at the inlet of the mesocosms was 0, and thus, the last term in equation (1) is equal

to 0, when we assume $P = 1$. The advective travel time, t_{ad}, to each sampling station was calculated from the distance of each sampling site from the inlet divided by the mean in-channel velocity, which was estimated from the measured discharge and the cross-sectional area of the surface water.

Raz to Rru transformation rates have been shown to be proportional to changes in oxygen, which is a common measurement of respiration rates [*González-Pinzón et al.*, 2012]. Therefore, estimated $k_{t_{ad}}$ can be used as a proxy of instantaneous rates of ecosystem respiration within the mesocosms. However, to compare Raz transformation values among mesocosms with different hydrologic conditions, we used the uptake velocity of Raz ($V_{f\text{-Raz}}$, mm min^{-1}), which was estimated by the product of $k_{t_{ad}}$ and the average mesocosm water depth. $V_{f\text{-Raz}}$ can be thought of as the effective velocity of the transformation of Raz into Rru [*Haggerty et al.*, 2014].

2.5. Hydrodynamic Model to Estimate Solute Transport, Retention, and Reactivity

A hydrodynamic model, the stochastic mobile-immobile model (SMIM), was used to independently characterize the flow dynamics of the three intensively instrumented mesocosms using the breakthrough curves of conductivity and Raz-Rru measured at the inlet of these mesocosms. SMIM is a probabilistic model that describes downstream transport as a distinct series of hydrological interactions between a mobile zone and an immobile zone [*Schumer et al.*, 2003; *Benson and Meerschaert*, 2009]. For this experimental setup, we consider the mobile zone as the preferential flow paths within the surface water, which may also include rapid interactions with the sediment-water interface. In addition, we consider that the immobile zone encompasses all transient storage areas, including both the slower-moving flow paths within the vegetated surface water and pore water transport through the sediment. SMIM is governed by an advection-dispersion equation, extended via a convolution integral with a memory function to represent storage in the system [*Boano et al.*, 2014], such that

$$\frac{\partial C(x,t)}{\partial t} = \int_0^t M\left(t - t'\right)\left[-v\frac{\partial C\left(x,t'\right)}{\partial x} + D\frac{\partial^2 C\left(x,t'\right)}{\partial x^2}\right]\mathrm{d}t' \tag{2}$$

where C is in stream concentration, t is time (s), x is downstream distance (m), $M(t)$ is the memory function, and v (m s^{-1}) and D (m^2 s^{-1}) are the velocity and dispersion coefficient, respectively. The memory function (equation (3)) depends on the distribution of waiting times between hydrologic interactions and represents the mass or number of particles immobilized at time t that remains immobile at a later time ($t + \mathrm{d}t$). The memory function is normally written in Laplace space, and it depends on $\tilde{\psi}(u)$ which describes solute transport via the immobile and mobile zones as follows:

$$\widetilde{M}(u) = u\bar{t}\frac{\widetilde{\psi}(u)}{1 - \widetilde{\psi}(u)} \tag{3}$$

$$\widetilde{\psi}(u) = \widetilde{\psi}_0[u + \Lambda - \Lambda\widetilde{\varphi}(u)] \tag{4}$$

where $\bar{t}$ is the average travel time in the mesocosm, defined as the mesocosm reach length divided by the velocity (v), $\widetilde{\psi}_0$ is the residence time distribution in the mobile zone, and $\widetilde{\phi}(u)$ is the residence time distribution in immobile zone. The Λ (s^{-1}) is the rate of solute exchange from the mobile zone into the immobile zone. We assume the solute residence times in the mobile zone followed an exponential distribution ($\psi_0(t) = e^{-t}$) and a heavy-tailed power law in the transient storage zones ($\varphi(t) \sim t^{-(1+\beta)}$) [*Haggerty et al.*, 2002; *Cardenas*, 2008]. Typically, a heavy-tailed power law has an infinite mean or variance, for exponents $0 < \beta < 1$, with the distribution of residence times being wider as β approaches 0. Therefore, the closer β is to 0, the longer it will take for the solute to move through the immobile zone and return to the mobile zone, which indicates longer residence times of the solute in the immobile zone. SMIM is virtually indistinguishable from a standard transient storage model [e.g., OTIS, *Runkel*, 1998] when the power law residence time distribution of solute within the immobile zone is replaced with an exponential distribution [*Stonedahl et al.*, 2012].

Characterization of solute transport and retention processes is improved when there is minimal truncation of the conservative tracer breakthrough data, which may occur from tracer sensitivity (i.e., signal-to-background noise) [*Drummond et al.*, 2012]. The sum of the concentrations of Raz and Rru throughout the injection was

used as an estimate of conservative solute transport within the mesocosm. For each in-stream Raz + Rru breakthrough curve, we estimated the residence time of the added tracers within the mesocosm by extending the tail of the breakthrough curve model output until the values returned to background concentrations of Raz + Rru. The mean arrival time (MAT) of the tracer to the sampling station was calculated from moment methods as $\frac{\int (Ct)dt}{\int Cdt}$ [*Luo et al*., 2006; *Ward et al*., 2013]. The input boundary condition was an 8.8 h injection of constant concentration at $x = 0$ and proceeded by zero concentration, and an initial concentration of zero everywhere else. The variation in the injection flow rate during the tracer injection was incorporated into the model input to improve the representation of the data.

To represent transformation of Raz to Rru within the SMIM model, a first-order reaction term was added within both the mobile and immobile zones by modifying equation (4) as follows [*Aubeneau et al*., 2015]:

$$\widetilde{\psi}_{\mathrm{Raz}}(u) = \widetilde{\psi}_{0,\ \mathrm{Raz}}[u + \Lambda - \Lambda\widetilde{\varphi}_{\mathrm{Raz}}(u)] \tag{5}$$

where the rate of exchange of Raz from the free-flowing water into the immobile zone is still represented by the conservative solute (Raz + Rru) rate of exchange, Λ (s^{-1}), but the residence time distribution of Raz within the mobile and immobile zones, $\widetilde{\psi}_{0,\ \mathrm{Raz}}$ and $\widetilde{\varphi}_{\mathrm{Raz}}$, is modified to include a first-order reaction term. The residence time distribution of Raz within the mobile zone is subject to the first-order transformation rate constant, k_{mob}, yielding $\psi_{0,\mathrm{Raz}}(t) = e^{-t}e^{-k_{\mathrm{mob}}t}$. The residence time distribution of Raz within the immobile zone is estimated from the conservative solute heavy-tailed power law subject to the first-order reaction rate, k_{imm}, yielding $\varphi_{\mathrm{Raz}}(t) \sim t^{-(1+\beta)}e^{-k_{\mathrm{imm}}t}$, with β the same power law slope from the Raz + Rru breakthrough curve model fit. Then, the Rru concentration was estimated by subtracting the model output of the Raz fit from the Raz + Rru fit.

2.6. Statistical Analysis

We used the nonparametric Spearman rank correlation coefficient to assess the relationships between the average hydraulic, sediment, and vegetation characteristics of the different mesocosms. A nonparametric Kruskal Wallis one-way analysis of variance test was used to examine whether there was a net effect of the acetate injection on $V_{f\text{-}\mathrm{Raz}}$ considering data from the eight mesocosms before and during the acetate portion of the tracer test. An analysis of covariance (ANCOVA) parallel lines model was used to compare the trend of $\ln(C_{\mathrm{Rru}}/C_{\mathrm{Raz}} + 1)$ from the longitudinal tracer profiles of Raz and Rru concentration during the plateau taken before and during the acetate portion of the tracer test to assess individual effects of acetate injection on each mesocosm. Moreover, Spearman correlations were used to explore the covariance between $V_{f\text{-}\mathrm{Raz}}$ and characteristics of the different mesocosms. We examined the relationship between $V_{f\text{-}\mathrm{Raz}}$ and the characteristics of the mesocosms by applying bivariate regression models (linear, exponential, power law, and logarithmic). Fits were performed by ordinary least squares, and the goodness of fit (R^2) was used for model selection [*Zar*, 2010]. We referred only to the best fit model in each case. In all cases, differences were considered statistically significant if $p < 0.05$. Statistical analysis was performed with MATLAB software version R2015b (The MathWorks, Inc., Natick, MA, USA).

3. Results

3.1. Physical, Hydraulic, and Vegetation Characterization

The distribution of vegetation and water varied among the mesocosms, as did the relative sediment volume (Figure 1 and Table 1). With the exception of the percentage unvegetated volume, all mesocosm parameters were significantly correlated to water depth ($p < 0.05$): discharge, bulk surface velocity, percentage vegetated area, and percentage vegetated volume were positively correlated, and the ratio of sediment volume to surface water volume was negatively correlated (Table 2). Submerged aquatic vegetation dominated the deeper mesocosms, with emergent vegetation, unvegetated surface water, and exposed sediment prevalent only in the shallower mesocosms, particularly in the shallowest riffle sections (Figure 1).

3.2. Daily Rates of Whole-Mesocosm Metabolism

The continuous DO concentration measurements in the three intensively monitored mesocosms showed clear diel cycles, with maximum DO concentrations between 12:00 and 13:00 (Figure 2a). Only GPP

Table 2. Spearman Correlations of Average Water Depth With Key Characteristics of the Vegetated Mesocosms

	Discharge	Velocity	Percent Vegetated Surface Water Area	Percent Vegetated Surface Water Volume	Sediment Volume: Surface Water Volume
r	0.91	0.80	0.92	0.99	-0.98
p	<0.05	<0.05	<0.05	<0.05	<0.05

correlated to the mesocosm parameters, decreasing with water depth (6.93, 3.74, and 2.71 g O_2 m^{-2} d^{-1} in 1-25, 2-10, and 3-07, respectively; Figure 2b). ER in mesocosm 3-07 was about half that of 1-25 and 2-10 (2.37 versus 5.39 and 5.51 g-O_2 m^{-2} d^{-1}, respectively; Figure 2b). As a result, NPP and *P*:*R* were highest in 1-25, lowest in 2-10, and moderate in 3-07 (NPP = 1.54, −1.77 and 0.35 g O_2 m^{-2} d^{-1}, respectively; *P*:*R* = 1.29, 0.68, and 1.15, respectively; Figure 2d), with the *P*:*R* following the same pattern.

3.3. Raz-Rru Transformation Rates

Cumulative Raz transformation to Rru increased with longitudinal distance in all mesocosms (Figure S1 in the supporting information). Raz to Rru transformation rates, $k_{t_{ad}}$, and the uptake velocity of Raz, $V_{f\text{-Raz}}$, varied by almost 3 orders of magnitude among the mesocosms (Table 3). $V_{f\text{-Raz}}$ was significantly correlated to all measured mesocosm parameters ($p < 0.05$) except the percentage unvegetated surface water volume. $V_{f\text{-Raz}}$ was positively correlated to water depth, discharge, velocity, percentage vegetated area, total volume, and percentage vegetated volume, and negatively correlated to the ratio of sediment volume to surface water volume (Figure 3 and Table 4).

Neither the $k_{\tau_{ad}}$ nor $V_{f\text{-Raz}}$ values from before or during the acetate injection were significantly different when considering all the mesocosms together (Kruskal Wallis test, $p = 0.60$), indicating that there was no consistent response to acetate across all mesocosms. However, the acetate injection did result in a statistically significant response in four of the individual mesocosms (3-07, 4-07, 2-10, and 6-35; ANCOVA *F* test, $p < 0.05$). Metabolic activity increased with acetate injection in all four mesocosms, representing the range of water depths. Because acetate had, on average, a small but positive effect on mesocosm metabolism, $k_{\tau_{ad}}$, $V_{f\text{-Raz}}$, and all resulting correlations were examined separately for preacetate and acetate data (Figure S1 and Tables 3 and 4).

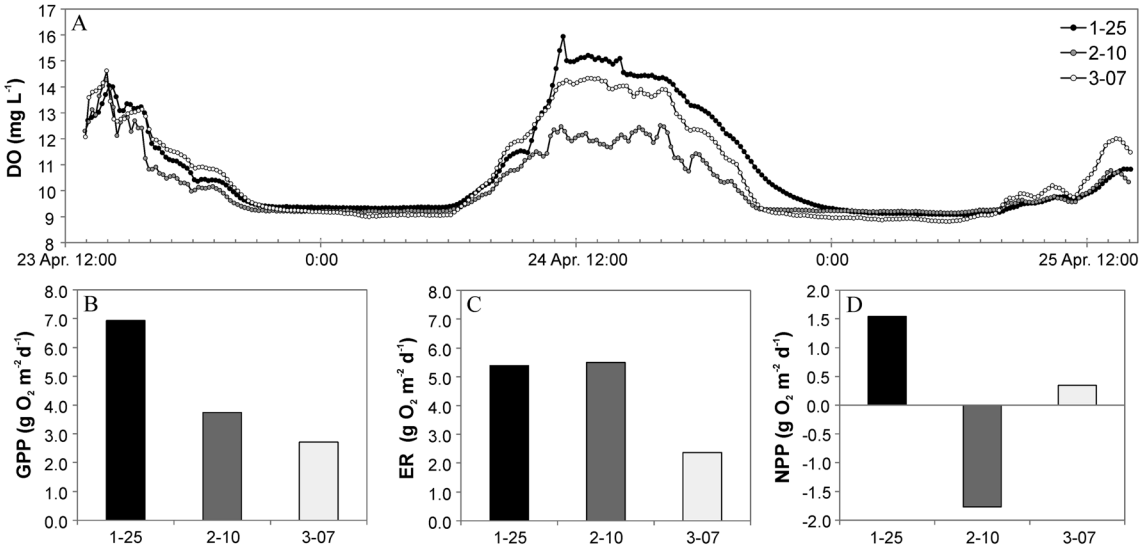

Figure 2. Whole-mesocosm metabolism estimated from the diel oxygen measurements. (a) Diel variation of DO for the three mesocosms representative of the different water column depth treatments. Daily rates of (b) gross primary production, (c) ecosystem respiration, and (d) net primary production for the three mesocosms differing in water column depth.

Table 3. Transformation Rates of the Hydrometabolic Tracer Raz in the Mesocosms Before and During the Acetate Injection[a]

Mesocosm Number	Preacetate			Acetate		
	$k_{t_{ad}}$ (h^{-1})	R^2	V_f -Raz (mm min^{-1})	$k_{t_{ad}}$ (h^{-1})	R^2	V_f-Raz (mm min^{-1})
3-07	0.06	0.88	0.03	0.15	0.92	0.08
4-07	2.17	0.27	1.37	3.43	0.27	2.17
2-10	0.67	0.78	0.80	1.34	0.77	1.61
9-10	0.91	0.94	0.95	0.90	0.11	0.94
1-25	1.18	0.90	4.60	0.89	0.91	3.46
12-25	1.61	0.98	5.69	2.16	0.85	7.63
6-35	1.18	0.97	6.14	2.99	0.94	15.55
10-35	4.98	0.88	25.90	4.98	0.61	25.90

[a]$k_{t_{ad}}$ is the Raz to Rru transformation rate determined from the slope of (ln (C_{Rru}/C_{Raz}) + 1 versus t_{ad}) (Figure S1), and $V_{f\text{-}Raz}$ is the uptake velocity, a proxy for ER within the vegetated mesocosms. R^2 values to determine $k_{t_{ad}}$ values are included.

3.4. Hydrodynamic Model for Solute Transport, Retention, and Reactivity

The hydrodynamic model was able to successfully reproduce the observed breakthrough curves on the basis of its conceptualization of hydrodynamic transport, retention, and reactivity, which considers hydrological interactions between a mobile and immobile zone (Figure 4 and Table 5). Despite the variation in hydrology

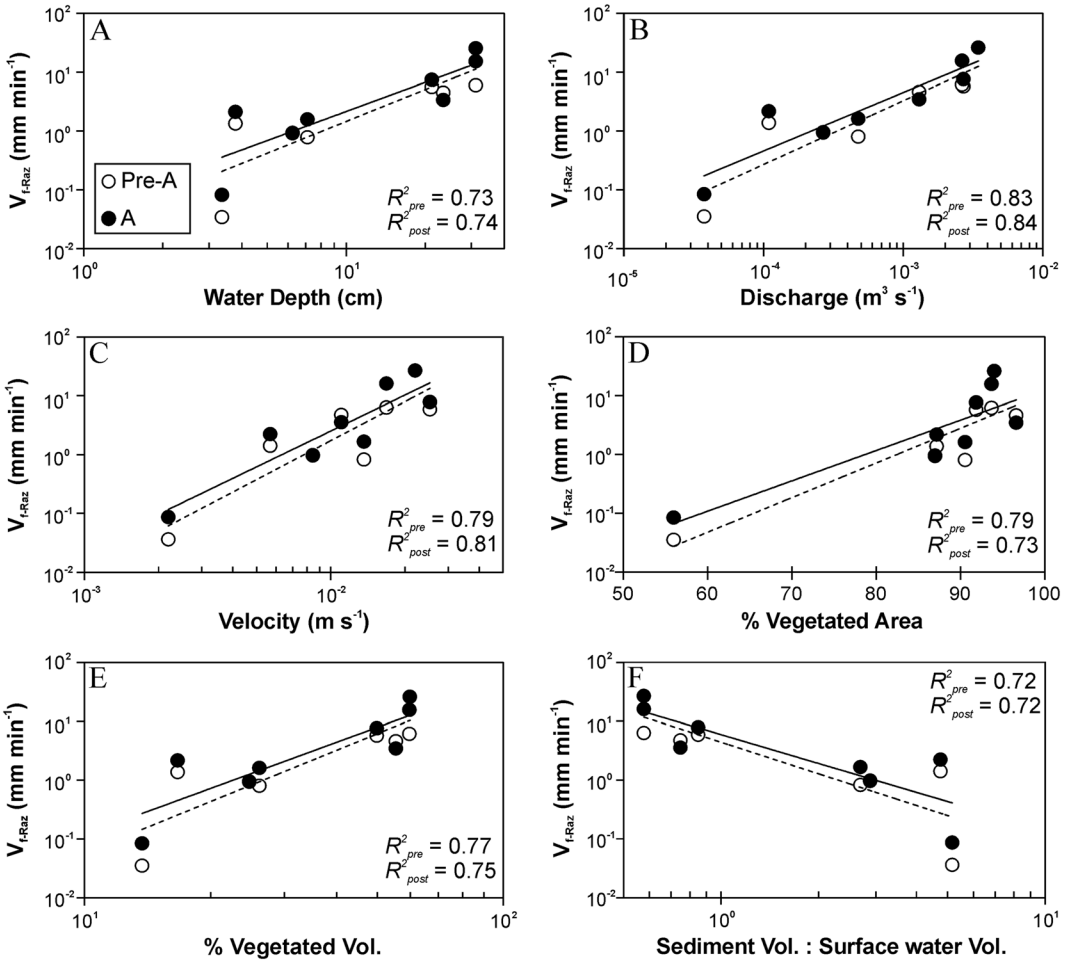

Figure 3. Uptake velocity ($V_{f\text{-}Raz}$) versus characteristics of vegetated mesocosms for before (white circles) and during (black circles) the acetate injection. The R^2 value for the best fit equation are shown for both before (dotted line) and during (solid line) the acetate injection. Plots are shown in semilog scale when the best fit equation was exponential and log-log scale when the best fit equation was power law.

Table 4. Spearman Correlations of Uptake Velocity ($V_{f\text{-Raz}}$) With Characteristics of the Vegetated Mesocosm, Before and During the Acetate Injection[a]

	Water Depth	Discharge	Velocity	Percent Vegetated Surface Water Area	Percent Vegetated Surface Water Volume	Sediment Volume: Surface Water Volume
				Preacetate		
r	0.88	0.88	0.76	0.76	0.88	-0.86
p	<0.05	<0.05	<0.05	<0.05	<0.05	<0.05
				Acetate		
r	0.90	0.90	0.81	0.79	0.90	-0.89
p	<0.05	<0.05	<0.05	<0.05	<0.05	<0.05

[a] $V_{f\text{-Raz}}$ is positively correlated to all characteristics except the ratio of sediment volume to surface water volume.

between the three mesocosm, a direct trend was not observed between water depth and model parameters estimated from the conservative (Raz + Rru) breakthrough curves. The velocity, dispersion, and mean arrival time were similar for the three mesocosms, while the solute exchange rate from mobile to immobile zones, Λ, was greatest within the shallowest mesocosm (3-07). Although β varied between the mesocosms, indicating a range of retention times within the transient storage zones, there was no clear trend between this value and the reactivity within the three mesocosms (i.e., to k_{mob}, k_{imm}, or $V_{f\text{-Raz}}$, Table 5).

The model was able to provide some additional information about the reactivity within the mobile and immobile zones from the fitted first-order transformation rates. In all cases the model better represented Raz and Rru data when reactivity was considered in both the mobile and immobile zones (Figure 5). Omitting reactivity within the immobile zone overestimated the concentration of Raz (Figure 5a) and underestimated the concentration of Rru within the tail of the breakthrough curve (Figure 5b). Furthermore, by adding reactivity within the mobile zone, the rising limb of the breakthrough curve was shifted and improved the Rru model fit. Values of k_{mob} were at least an order of magnitude higher than values of k_{imm} in all three mesocosms (Table 5).

4. Discussion

4.1. Hydrologic and Vegetation Controls on Metabolism

Our results demonstrate that stream water depth, aquatic vegetation abundance, and metabolic activity are highly correlated under low flow conditions, and, as such, that aquatic vegetation beds can significantly contribute to metabolically active transient storage in streams. The correlation between stream flow and aquatic vegetation is well demonstrated in the literature. Aquatic vegetation cover and biomass are typically negatively correlated with flow and water depth [*Dawson*, 1976; *Flynn et al*., 2002] when compared across a broad range of flow and depth conditions (0.2–1.3 m^{-3} s and 0.5–3 m, respectively). However, macrophyte cover has been shown to be positively correlated with flow and depth in lowland stream environments analogous to our mesocosms, with stable, low flow conditions (velocity < 0.4 m s^{-1} and/or shallow water depth < 0.7 m) [*Wilby et al*., 1998; *Bunn and Arthington*, 2002; *Riis and Biggs*, 2003; *Riis et al*., 2008]. In these systems, increases in discharge are more reflected in increases in water column depth than in water velocity, providing additional habitat for aquatic vegetation rather than vegetation-scouring flows. Further, at velocities below <0.005–0.06 m s^{-1}, within the range of our mesocosms, growth rates of both vascular vegetation and algae have been shown to be positively correlated to velocity due to decreasing diffusive boundary layer thickness and associated nutrient limitation [*Hurd*, 2000; *Koch*, 2001]. The positive correlation between vegetation cover, flow, and water depth is particularly evident during low flow periods caused by drought or water abstraction [*Wright and Berrie*, 1987].

The link between aquatic vegetation and characteristics of ecosystem function, in particular metabolic activity, in streams has been receiving increased attention [*O'Brien et al*., 2013; *Levi et al*., 2015; *Alnoee et al*., 2016]; however, the link between stream flow, vegetation abundance, and function has not been explicitly identified in lotic systems previously. Aquatic vegetation is known to influence stream nutrient dynamics and autotrophic metabolism via a number of mechanisms. These include primary production and nutrient assimilation

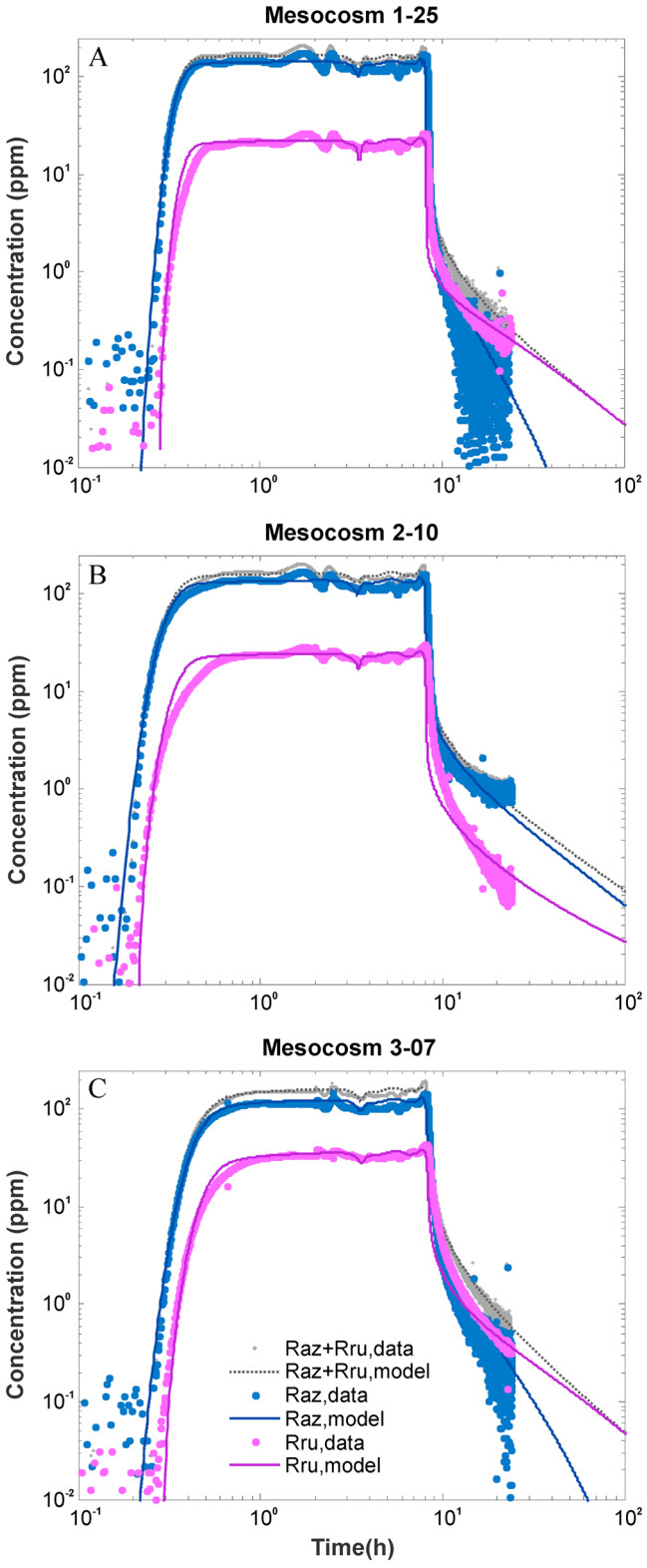

Figure 4. Breakthrough curves of resazurin (Raz), Resorufin (Rru), and conservative (Raz + Rru) tracer concentrations (points) and model fits (lines) measured at the outlet of the mesocosms 1-25 (A), 2-10 (B) and 3-07 (C) during the Raz constant rate injection. Hydrodynamic model parameters from model fit are shown in Table 3.

by the plants themselves and by epiphytic communities, increased retention of nutrients sorbed to accumulated sediments and particulate organic matter, and by linking nutrient cycling between the water column and bed sediments [*Clarke*, 2002; *O'Brien et al*., 2013, and references therein]. Likewise, aquatic vegetation abundance may stimulate heterotrophic metabolism by providing substrate for epiphytic biofilms in the water column, and by supplying and trapping organic matter. A literature review by *Alnoee et al.* [2016] showed positive correlations between autotrophic biomass and primary production and respiration, while *O'Brien et al.* [2013] found that primary production, but not ecosystem respiration, was closely correlated with macrophyte cover. Our results of daily rates of GPP agree with these findings, with higher rates in mesocosms with higher water depths and coverage of aquatic vegetation (Figure 2). In addition, ER was lowest in the mesocosm with the lowest vegetation coverage, suggesting an influence of aquatic vegetation on ER. This was further supported by the positive correlations between $V_{f\text{-Raz}}$ and vegetation abundance when considering data from the 8 mesocosms. Our result is consistent with *Haggerty et al.* [2014], who showed that $V_{f\text{-Raz}}$ increased with increasing biofilm biomass as well as surface flow heterogeneity.

While we found a strong correlation between ER, inferred from $V_{f\text{-Raz}}$, and water depth in the mesocosms, we also found that daily rates of ER measured from diel DO concentration time series did not scale perfectly with water depth in the three intensively studied mesocosms. This discrepancy highlights some of the potential differences between values derived from the two methods. Both the diel DO and Raz to Rru transformation methods are, in theory,

Table 5. Hydrodynamic Model Parameters for Conservative (Raz + Rru), Raz and Rru Breakthrough Curves (BTCs) in Mesocosms 1-25, 2-10, and 3-07[a]

Mesocosm Number	Average Water Depth (cm)	Velocity [b] ($m\,s^{-1}$)	Dispersion [b] ($m^2\,s$)	λ [b] (s^{-1})	β [b]	MAT [b] (h)	k_{mob} [c] (h^{-1})	k_{imm} [c] (h^{-1})
3-07	3.4	9.50×10^{-3}	2.70×10^{-3}	9.80×10^{-3}	0.55	5.5	1.58	0.036
2-10	7.2	1.30×10^{-2}	3.50×10^{-3}	1.00×10^{-3}	0.28	6.1	1.44	0.002
1-25	23.4	1.20×10^{-2}	1.30×10^{-3}	1.10×10^{-3}	0.40	4.7	1.80	0.072

[a]As estimated from the conservative (Raz + Rru) BTCs, λ is the rate of solute exchange from the mobile to immobile zone, β is the slope of the power law residence time distribution within the immobile zone with values closer to 0 indicating increased solute retention ($t^{(1+\beta)}$, $0<\beta<1$), and the mean arrival time (MAT) is the first moment of the conservative (Raz + Rru) model fit. As estimated from the Raz and Rru BTCs, k_{mob} and k_{imm} are the first-order transformation rates within the mobile and immobile zone, respectively.
[b]Estimated from the conservative (Raz + Rru) BTCs.
[c]Estimated from the Raz and Rru BTCs.

sensitive to aerobic respiration of stream ecosystems; the diel DO method measures the net effects of all oxygen producing and consuming organisms in the ecosystem, while Raz transformation is the result of the reducing conditions produced by oxygen consumption within the ecosystem. Raz transformation has been clearly correlated to oxygen consumption in batch and in situ stream experiments [*González-Pinzón*

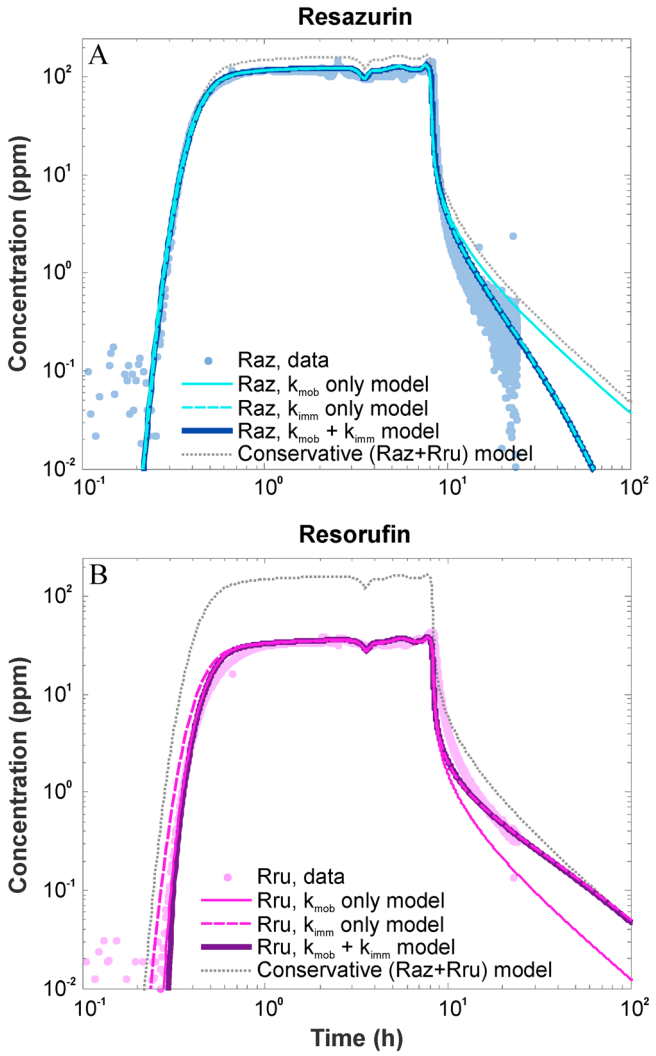

Figure 5. Example of model fits of (a) Raz and (b) Rru BTCs produced when accounting for reactivity within only the mobile zone (k_{mob}), only the immobile zone (k_{imm}), or within both zones (as in Figure 4). The modeled conservative (Raz + Rru) BTC is shown for reference. Example data are from mesocosm 3-07.

et al., 2012] and more generally to diel DO-based ER estimates [*Argerich et al*., 2011]. However, substantial comparison of the two approaches has yet to be made. Notably, the two approaches measured respiration at different timescales. Daily rates of ER based on diel DO changes are integrated measurements over 24 h based on consideration that average instantaneous rates during nighttime are also representative of daytime rates. In contrast, Raz transformation provides information on instantaneous rates of respiration at the time of measurement, in our case midafternoon. Raz-based rates of ecosystem respiration have been shown to be relatively constant during day and night [*González-Pinzón et al*., 2015]. The Raz technique is notable in that it provides an instantaneous measurement method with which to disentangle metabolic activity at any given time of day. Despite this, more information is needed from a broader variety of streams and under different temporal conditions to ensure this trend is consistent.

4.2. Vegetation Beds Are Metabolically Active Transient Storage Zones

The wide range of $V_{f\text{-Raz}}$ values found across the eight mesocosms (0.03–25.90 mm min^{-1}; Table 3) not only cover but exceed, by almost 2 orders of magnitude, the range of values previously reported for natural and artificial stream systems. *Argerich et al.* [2011] reported $V_{f\text{-Raz}}$ values of 0.036–0.28 mm min^{-1} in two morphologically contrasting reaches of the same stream dominated by bedrock and alluvial substrata, respectively, while *Haggerty et al.* [2009] observed $V_{f\text{-Raz}}$ values of 0.69 mm min^{-1} in April in a second-order forested stream in Spain. In flumes with variable bed form geometry and biofilm biomass, *Haggerty et al.* [2014] reported $V_{f\text{-Raz}}$ values of 0.013–0.030 mm min^{-1}. The wide range of $V_{f\text{-Raz}}$ values and strong correlation to vegetation abundance observed in this study suggest that aquatic vegetation and, more specifically, the abundance of aquatic vegetation can have a substantial effect on metabolic activity within lowland streams. Furthermore, our results suggest that aquatic vegetation in lowland streams can support respiration rates as high as, if not higher, than the majority of those observed in steams where the hyporheic zone and benthic biofilms are the major metabolically active compartment contributing to whole-system metabolic activity. Unfortunately, our study is not able to directly distinguish the relative importance to observed metabolic activity of the contribution of the aquatic vegetation itself from that of associated epiphytic biofilms, nor the relative importance of the vegetated surface water from that of hyporheic sediments. Nevertheless, stream sections dominated by aquatic vegetation have been shown to have higher metabolic activity than those dominated by sediment, in large part due to epiphytic biofilms associated with the vegetation [*Alnoee et al*., 2016]. Given the high surface area of *Ranunculus*, the dominant vegetation type in our mesocosms, the contribution of epiphytes to observed metabolic activity could likewise be high. The fact that mesocosm metabolic activity was inversely correlated with the ratio of sediment volume to surface water volume does indicate that the vegetated surface water, and not the bed sediments, had a greater influence on metabolic activity.

The continuous tracer breakthrough curves in the three highly instrumented mesocosms provide additional insight into the relative importance of different transport pathways (i.e., relatively fast or slow water movement) along the mesocosms on the metabolic activity. Our hydrodynamic model identified two zones, referred to as mobile and immobile, which we assumed were associated with the quicker transport through the surface water and the slower transport through transient storage zones, respectively. Both slower transport flow paths through vegetated surface water and within hyporheic sediments could contribute to transient storage in this system. In all cases, the model fit to the reactive tracer time series was improved when reactive terms were applied to both zones, suggesting that both the aquatic vegetation and the sediments contribute to metabolically active transient storage within these systems. Moreover, we found that the modeled reaction rates within the mobile zone are an order of magnitude higher than in the immobile zone, suggesting that the contribution to metabolic activity within the vegetation in the water column is considerably higher than that in sediments. The model indicated that all mesocosms had high hydrological retention (i.e., a mean arrival time of ~5 h or more and wide power law residence time distributions). Also, there was no direct trend between hydrologic retention parameters (i.e., to β, MAT) and estimates of reactivity (i.e., to k_{mob}, k_{imm}, $V_{f\text{-Raz-mob}}$, or $V_{f\text{-Raz}}$). Hence, it is not the lack of hydrologic retention within the shallow mesocosms that results in lower metabolic activity. Rather, that metabolic activity is higher in the flow within the vegetated surface water than in the transient storage zones. A likely explanation for the increased metabolic activity within the mobile zone is the abundance of epiphytic biofilm present on vegetation that promotes fast reactivity, supporting previous findings where metabolically active storage zones were not related to water transient storage size, but rather to areas with high biomass [*Argerich et al*., 2011].

Overall, model results were consistent with the observed positive correlation between transformation rates and vegetation abundance seen in all mesocosms. The modeled mobile zone reaction rates are similar to the observed Raz-based $k_{t_{ad}}$ values. A possible explanation for differences between modeled and data-calculated reaction rates may be due to the fact that the model that assumes the reaction rate within each zone is homogeneous. Spatial heterogeneity in reaction rates within transient storage zones, along preferential flowpaths, or within the benthic (interfacial) zone and/or microzones [*Briggs et al*., 2015], would allow for higher maximum rates. Such spatial heterogeneity in the form of anoxic sediment zones would be particularly critical to Raz transformation, as, theoretically, Raz only transforms under aerobic conditions. Incorporation of spatial heterogeneity in reaction rates within transient storage zones, either within surface water column or in hyporheic sediments, is a promising direction for future research to improve our understanding of Raz-Rru transformation within streams.

4.3. Effects of Acetate Injection

The injection of acetate, a labile carbon source, to test if metabolic activity was stimulated in the mesocosms within a time frame of a few hours did not yield a consistent response in $k_{\tau_{ad}}$ and $V_{f\text{-Raz}}$ values across the mesocosms. The four mesocosms that had a statistically significant response, representing the range of water depths, exhibited higher acetate $k_{\tau_{ad}}$ and $V_{f\text{-Raz}}$ values (Tables 3 and 4), suggesting that acetate had on average a slight positive effect on metabolic activity. The lack of a consistent, significant response to acetate could be because the mesocosm ecosystems were not carbon limited, because 2 h was not enough time for the ecosystem to respond to the added carbon, or that acetate was not the most bioreactive carbon source for the microbial assemblages present in the mesocosms. Heterotrophic metabolism is often carbon limited, hence adding a labile carbon source generally increases respiration [*Bernhardt and Likens*, 2002; *Johnson et al*., 2012], but not always [*Baker et al*., 2000; *Craft et al*., 2002]. Within our mesocosms, the positive NPP values (except in 2-10), abundance of vegetation biomass, low velocities, and steady state conditions provide possible evidence against carbon limitation. Alternatively, the acetate could have stimulated anaerobic microbial respiration [*Baker et al*., 1999], to which Raz transformation is not, theoretically, sensitive. However, significant changes in anaerobic respiration would be less expected in our system, given the high oxygen concentrations measured in the mesocosms and the shallow depth of the sediments.

4.4. Implications for Ecosystem Function in Lowland Rivers

Our results demonstrate that ecosystem function, in the form of metabolic activity, is highly correlated to stream water depth and abundance of submerged vegetation under low flow conditions. These findings suggest important implications for how ecosystem function in lowland rivers would respond to climate change-induced drought, human water abstraction, or other changes that result in reduced stream flows. Groundwater-dominated lowland chalk aquifer streams, which our mesocosms were designed to be representative of, are characterized by stable flow, intermittently drying upper reaches, and high coverage of aquatic vegetation dominated by *Ranunculus* spp. The importance of chalk streams is reflected in their being designated habitats within the UK Biodiversity Action Plan and associated *Ranunculus* spp. beds as a priority habitat under the European Union's Habitats Directive [*Westwood et al*., 2006, and references therein]. Climate change is predicted to result in increased seasonal and annual flow variability, with lower groundwater levels and water abstractions contributing to decreased stream flow, particularly in the summer [*Westwood et al*., 2006, and references therein; *Lavers et al*., 2015]. Our results illustrate the importance of maintaining sufficient flow and vegetation cover in order to optimize stream ecosystem function [*Champion and Tanner*, 2000; *Acreman and Ferguson*, 2010].

There is a need to improve our understanding of the factors governing vegetation dynamics in lowland systems to better evaluate and manage their susceptibility to changes in environmental conditions, including projected patterns of climate variability and continued water abstraction [*Flynn et al*., 2002; *Franklin et al*., 2008; *Bornette and Puijalon*, 2010; *Wilby et al*., 2010]. One challenge to this is separating the effects of multiple stressors (e.g., modified flow versus associated land use changes) on biotic responses to inform effective management of water resources and ecological health [*Bunn and Arthington*, 2002]. Our mesocosm experiment provides a basis to approach these questions, by providing information on the effect of flow and water depth without associated changes in water quality or temporal flow variability. Further work is needed to corroborate our results with field studies and to establish the mechanisms driving the correlations between flow-controlled patterns in aquatic vegetation and in ecosystem functions, such as metabolism.

5. Conclusions

It is well recognized that stream flow variation has a major control on stream aquatic vegetation, including biodiversity, abundance, and growth patterns, with reduced flows being linked to declining abundance of aquatic vegetation, especially in lowland streams. However, few studies have linked changes in vegetation dynamics to changes in ecosystem function, and none in relation to water depth or flow. Our results demonstrate that under stable, low flow conditions, changes in water level and discharge are positively correlated to aquatic vegetation cover and ecosystem respiration. Most notably, our results suggest that submerged aquatic vegetation can have a remarkable influence on reactivity rates in the water column, indicating that vegetation beds are significant sites of metabolically active transient storage in streams. These results further support the importance of maintaining minimum flows in lowland streams to sustain aquatic vegetation and optimize stream ecosystem function.

Acknowledgments

The authors thank the DRI-STREAM mesocosm facility and Fobdown Watercress Farm for the use of their facilities, the entire Leverhulme Hyporheic Zone Network Team for their support and insight, and the Editor and anonymous reviewer for their help to improve this manuscript. Financial support for the experiment was provided by The Leverhulme Trust through the project "Where rivers, groundwater and disciplines meet: A hyporheic research network" and from the authors' institutions. All data provided in this study may be obtained by contacting the corresponding author at marie.kurz@drexel.edu.

References

Acreman, M. C., and A. J. D. Ferguson (2010), Environmental flows and the European Water Framework Directive, *Freshw. Biol.*, *55*(1), 32–48, doi:10.1111/j.1365-2427.2009.02181.x.

Acreman, M. C., I. C. Overton, J. King, P. J. Wood, I. G. Cowx, M. J. Dunbar, E. Kendy, and W. J. Young (2014), The changing role of ecohydrological science in guiding environmental flows, *Hydrol. Sci. J.*, *59*(3–4), 433–450, doi:10.1080/02626667.2014.886019.

Alexander, R. B., J. K. Böhlke, E. W. Boyer, M. B. David, J. W. Harvey, P. J. Mulholland, S. P. Seitzinger, C. R. Tobias, C. Tonitto, and W. M. Wollheim (2009), Dynamic modeling of nitrogen losses in river networks unravels the coupled effects of hydrological and biogeochemical processes, *Biogeochemistry*, *93*(1–2), 91–116, doi:10.1007/s10533-008-9274-8.

Alnoee, A. B., T. Riis, and A. Baattrup-Pedersen (2016), Comparison of metabolic rates among macrophyte and nonmacrophyte habitats in streams, *Freshw. Sci.*, *35*(3), 834–844, doi:10.1086/687842.

Argerich, A., R. Haggerty, E. Martí, F. Sabater, and J. Zarnetske (2011), Quantification of metabolically active transient storage (MATS) in two reaches with contrasting transient storage and ecosystem respiration, *J. Geophys. Res.*, *116*, G03034, doi:10.1029/2010JG001379.

Arroita, M., I. Aristi, J. Díez, M. Martinez, G. Oyarzun, and A. Elosegi (2015), Impact of water abstraction on storage and breakdown of coarse organic matter in mountain streams, *Sci. Total Environ.*, *503–504*, 233–240, doi:10.1016/j.scitotenv.2014.06.124.

Aubeneau, A. F., J. D. Drummond, R. Schumer, D. Bolster, J. L. Tank, and A. I. Packman (2015), Effects of benthic and hyporheic reactive transport on breakthrough curves, *Freshw. Sci.*, *34*(1), 301–315, doi:10.1086/680037.

Baker, M. A., C. N. Dahm, and H. M. Valett (1999), Acetate retention and metabolism in the hyporheic zone of a mountain stream, *Limnol. Oceanogr.*, *44*(6), 1530–1539, doi:10.4319/lo.1999.44.6.1530.

Baker, M. A., H. M. Valett, and C. N. Dahm (2000), Organic carbon supply and metabolism in a shallow groundwater ecosystem, *Ecology*, *81*(11), 3133–3148, doi:10.1890/0012-9658(2000)081[3133:OCSAMI]2.0.CO;2.

Battin, T. J., L. A. Kaplan, S. Findlay, C. S. Hopkinson, E. Marti, A. I. Packman, J. D. Newbold, and F. Sabater (2008), Biophysical controls on organic carbon fluxes in fluvial networks, *Nat. Geosci.*, *1*(2), 95–100, doi:10.1038/ngeo101.

Bencala, K. E., and R. A. Walters (1983), Simulation of solute transport in a mountain pool-and-riffle stream: A transient storage model, *Water Resour. Res.*, *19*(3), 718–724, doi:10.1029/WR019i003p00718.

Benson, D. A., and M. M. Meerschaert (2009), A simple and efficient random walk solution of multi-rate mobile/immobile mass transport equations, *Adv. Water Resour.*, *32*(4), 532–539, doi:10.1016/j.advwatres.2009.01.002.

Bernhardt, E. S., and G. E. Likens (2002), Dissolved organic carbon enrichment alters nitrogen dynamics in a forest stream, *Ecology*, *83*(6), 1689–1700, doi:10.1890/0012-9658(2002)083[1689:DOCEAN]2.0.CO;2.

Boano, F., J. W. Harvey, A. Marion, A. I. Packman, R. Revelli, L. Ridolfi, and A. Wörman (2014), Hyporheic flow and transport processes: Mechanisms, models, and biogeochemical implications, *Rev. Geophys.*, *52*, 603–679, doi:10.1002/2012RG000417.

Bornette, G., and S. Puijalon (2010), Response of aquatic plants to abiotic factors: A review, *Aquat. Sci.*, *73*(1), 1–14, doi:10.1007/s00027-010-0162-7.

Bott, T. L. (1996), Primary productivity and community respiration, in *Methods in Stream Ecology*, pp. 533–556, Academic Press, San Diego, Calif.

Briggs, M. A., F. D. Day-Lewis, J. P. Zarnetske, and J. W. Harvey (2015), A physical explanation for the development of redox microzones in hyporheic flow, *Geophys. Res. Lett.*, *42*, 4402–4410, doi:10.1002/2015GL064200.

Bunn, S. E., and A. H. Arthington (2002), Basic principles and ecological consequences of altered flow regimes for aquatic biodiversity, *Environ. Manage.*, *30*(4), 492–507, doi:10.1007/s00267-002-2737-0.

Cardenas, M. B. (2008), Surface water-groundwater interface geomorphology leads to scaling of residence times, *Geophys. Res. Lett.*, *35*, L08402, doi:10.1029/2008GL033753.

Champion, P. D., and C. C. Tanner (2000), Seasonality of macrophytes and interaction with flow in a New Zealand lowland stream, *Hydrobiologia*, *441*(1), 1–12, doi:10.1023/A:1017517303221.

Clarke, S. J. (2002), Vegetation growth in rivers: Influences upon sediment and nutrient dynamics, *Prog. Phys. Geogr.*, *26*(2), 159–172, doi:10.1191/0309133302pp324ra.

Craft, J. A., J. A. Stanford, and M. Pusch (2002), Microbial respiration within a floodplain aquifer of a large gravel-bed river, *Freshw. Biol.*, *47*(2), 251–261, doi:10.1046/j.1365-2427.2002.00803.x.

Dahm, C. N., M. A. Baker, D. I. Moore, and J. R. Thibault (2003), Coupled biogeochemical and hydrological responses of streams and rivers to drought, *Freshw. Biol.*, *48*(7), 1219–1231, doi:10.1046/j.1365-2427.2003.01082.x.

Dawson, F. H. (1976), The annual production of the aquatic macrophyte *Ranunculus penicillatus* var. *Calcareus* (R.W. Butcher) C.D.K. Cook, *Aquat. Bot.*, *2*, 51–73, doi:10.1016/0304-3770(76)90007-3.

Drummond, J. D., T. P. Covino, A. F. Aubeneau, D. Leong, S. Patil, R. Schumer, and A. I. Packman (2012), Effects of solute breakthrough curve tail truncation on residence time estimates: A synthesis of solute tracer injection studies, *J. Geophys. Res.*, *117*, G00N08, doi:10.1029/2012JG002019.

Drummond, J. D., R. J. Davies-Colley, R. Stott, J. P. Sukias, J. W. Nagels, A. Sharp, and A. I. Packman (2014), Retention and remobilization dynamics of fine particles and microorganisms in pastoral streams, *Water Res.*, *66*, 459–472, doi:10.1016/j.watres.2014.08.025.

Drummond, J. D., S. Bernal, D. von Schiller, and E. Marti (2016), Linking in-stream nutrient uptake to hydrologic retention in two headwater streams, *Freshw. Sci.*, *35*(4), 1176–1188, doi:10.1086/688599.

Ensign, S. H., and M. W. Doyle (2005), In-channel transient storage and associated nutrient retention: Evidence from experimental manipulations, *Limnol. Oceanogr.*, *50*(6), 1740–1751, doi:10.4319/lo.2005.50.6.1740.

Fellows, C. S., J. E. Clapcott, J. W. Udy, S. E. Bunn, B. D. Harch, M. J. Smith, and P. M. Davies (2006), Benthic metabolism as an indicator of stream ecosystem health, *Hydrobiologia*, *572*(1), 71–87, doi:10.1007/s10750-005-9001-6.

Flynn, N. J., D. L. Snook, A. J. Wade, and H. P. Jarvie (2002), Macrophyte and periphyton dynamics in a UK Cretaceous chalk stream: The River Kennet, a tributary of the Thames, *Sci. Total Environ.*, *282–283*, 143–157, doi:10.1016/S0048-9697(01)00949-4.

Franklin, P., M. Dunbar, and P. Whitehead (2008), Flow controls on lowland river macrophytes: A review, *Sci. Total Environ.*, *400*(1–3), 369–378, doi:10.1016/j.scitotenv.2008.06.018.

French, T. D., and P. A. Chambers (1997), Reducing flows in the Nechako River (British Columbia, Canada): Potential response of the macrophyte community, *Can. J. Fish. Aquat. Sci.*, *54*(10), 2247–2254, doi:10.1139/f97-133.

González-Pinzón, R., R. Haggerty, and D. D. Myrold (2012), Measuring aerobic respiration in stream ecosystems using the resazurin-resorufin system, *J. Geophys. Res.*, *117*, G00N06, doi:10.1029/2012JG001965.

González-Pinzón, R., H. Roy, and A. Argerich (2014), Quantifying spatial differences in metabolism in headwater streams, *Freshw. Sci.*, *33*(3), 798–811, doi:10.1086/677555.

González-Pinzón, R., M. Peipoch, R. Haggerty, E. Martí, and J. H. Fleckenstein (2015), Nighttime and daytime respiration in a headwater stream, *Ecohydrology*, *9*, 93–100, doi:10.1002/eco.1615.

Gurnell, A. (2014), Plants as river system engineers, *Earth Surf. Process. Landf.*, *39*(1), 4–25, doi:10.1002/esp.3397.

Haggerty, R. (2013), Analytical solution and simplified analysis of coupled parent-daughter steady-state transport with multirate mass transfer, *Water Resour. Res.*, *49*, 635–639, doi:10.1029/2012WR012821.

Haggerty, R., S. M. Wondzell, and M. A. Johnson (2002), Power-law residence time distribution in the hyporheic zone of a 2nd-order mountain stream, *Geophys. Res. Lett.*, *29*(13), 18–1, doi:10.1029/2002GL014743.

Haggerty, R., A. Argerich, and E. Martı (2008), Development of a "smart" tracer for the assessment of microbiological activity and sediment-water interaction in natural waters: The resazurin-resorufin system, *Water Resour. Res.*, *44*, W00D01, doi:10.1029/2007WR006670.

Haggerty, R., E. Martí, A. Argerich, D. von Schiller, and N. B. Grimm (2009), Resazurin as a "smart" tracer for quantifying metabolically active transient storage in stream ecosystems, *J. Geophys. Res.*, *114*, G03014, doi:10.1029/2008JG000942.

Haggerty, R., M. Ribot, G. A. Singer, E. Martí, A. Argerich, G. Agell, and T. J. Battin (2014), Ecosystem respiration increases with biofilm growth and bed forms: Flume measurements with resazurin, *J. Geophys. Res. Biogeosci.*, *119*, 220–2230, doi:10.1002/2013JG002498.

Hurd, C. L. (2000), Water motion, marine macroalgal physiology, and production, *J. Phycol.*, *36*(3), 453–472, doi:10.1046/j.1529-8817.2000.99139.x.

James, A. B. W., Z. S. Dewson, and R. G. Death (2008), The effect of experimental flow reductions on macroinvertebrate drift in natural and streamside channels, *River Res. Appl.*, *24*(1), 22–35, doi:10.1002/rra.1052.

Johnson, L. T., T. V. Royer, J. M. Edgerton, and L. G. Leff (2012), Manipulation of the dissolved organic carbon pool in an agricultural stream: Responses in microbial community structure, denitrification, and assimilatory nitrogen uptake, *Ecosystems*, *15*(6), 1027–1038, doi:10.1007/s10021-012-9563-x.

Kleeberg, A., J. Köhler, T. Sukhodolova, and A. Sukhodolov (2010), Effects of aquatic macrophytes on organic matter deposition, resuspension and phosphorus entrainment in a lowland river, *Freshw. Biol.*, *55*(2), 326–345, doi:10.1111/j.1365-2427.2009.02277.x.

Koch, E. W. (2001), Beyond light: Physical, geological, and geochemical parameters as possible submersed aquatic vegetation habitat requirements, *Estuaries*, *24*(1), 1–17, doi:10.2307/1352808.

Laizé, C. L. R., M. C. Acreman, C. Schneider, M. J. Dunbar, H. A. Houghton-Carr, M. Flörke, and D. M. Hannah (2014), Projected flow alteration and ecological risk for Pan-European rivers, *River Res. Appl.*, *30*(3), 299–314, doi:10.1002/rra.2645.

Lake, P. S. (2003), Ecological effects of perturbation by drought in flowing waters, *Freshw. Biol.*, *48*(7), 1161–1172, doi:10.1046/j.1365-2427.2003.01086.x.

Lavers, D. A., D. M. Hannah, and C. Bradley (2015), Connecting large-scale atmospheric circulation, river flow and groundwater levels in a chalk catchment in southern England, *J. Hydrol.*, *523*, 179–189, doi:10.1016/j.jhydrol.2015.01.060.

Levi, P. S., T. Riis, A. B. Alnøe, M. Peipoch, K. Maetzke, C. Bruus, and A. Baattrup-Pedersen (2015), Macrophyte complexity controls nutrient uptake in lowland streams, *Ecosystems*, *18*(5), 914–931, doi:10.1007/s10021-015-9872-y.

Luo, J., O. A. Cirpka, and P. K. Kitanidis (2006), Temporal-moment matching for truncated breakthrough curves for step or step-pulse injection, *Adv. Water Resour.*, *29*(9), 1306–1313, doi:10.1016/j.advwatres.2005.10.005.

Mulholland, P. J., C. S. Fellows, J. L. Tank, N. B. Grimm, J. R. Webster, S. K. Hamilton, E. Martí, L. Ashkenas, W. B. Bowden, and W. K. Dodds (2001), Inter-biome comparison of factors controlling stream metabolism, *Freshw. Biol.*, *46*(11), 1503–1517.

O'Brien, J. M., J. L. Lessard, D. Plew, S. E. Graham, and A. R. McIntosh (2013), Aquatic macrophytes alter metabolism and nutrient cycling in lowland streams, *Ecosystems*, *17*(3), 405–417, doi:10.1007/s10021-013-9730-8.

Peipoch, M., E. Gacia, A. Pastor, M. Ribot, J. L. Riera, F. Sabater, and E. Martí (2014), Intrinsic and extrinsic drivers of autotrophic nitrogen cycling in stream ecosystems: Results from a translocation experiment, *Limnol. Oceanogr.*, *59*(6), 1973–1986, doi:10.4319/lo.2014.59.6.1973.

Phillips, E. C. (2003), Habitat preference of aquatic macroinvertebrates in an east Texas sandy stream, *J. Freshw. Ecol.*, *18*(1), 1–11, doi:10.1080/02705060.2003.9663946.

Poff, N. L., J. D. Allan, M. B. Bain, J. R. Karr, K. L. Prestegaard, B. D. Richter, R. E. Sparks, and J. C. Stromberg (1997), The natural flow regime, *BioScience*, *47*(11), 769–784, doi:10.2307/1313099.

Rajwa-Kuligiewicz, A., R. J. Bialik, and P. M. Rowiński (2015), Dissolved oxygen and water temperature dynamics in lowland rivers over various timescales, *J. Hydrol. Hydromech.*, *63*(4), 353–363, doi:10.1515/johh-2015-0041.

Riis, T., and B. J. F. Biggs (2003), Hydrologic and hydraulic control of macrophyte establishment and performance in streams, *Limnol. Oceanogr.*, *48*(4), 1488–1497, doi:10.4319/lo.2003.48.4.1488.

Riis, T., A. M. Suren, B. Clausen, and K. Sand-Jensen (2008), Vegetation and flow regime in lowland streams, *Freshw. Biol.*, *53*(8), 1531–1543, doi:10.1111/j.1365-2427.2008.01987.x.

Riis, T., W. K. Dodds, P. B. Kristensen, and A. J. Baisner (2012), Nitrogen cycling and dynamics in a macrophyte-rich stream as determined by a release, *Freshw. Biol.*, *57*(8), 1579–1591, doi:10.1111/j.1365-2427.2012.02819.x.

Runkel, R. L. (1998), One-dimensional transport with inflow and storage (OTIS): A solute transport model for streams and rivers, U.S. Geol. Surv. Water-Resour. Invest. Rep. 98-4018, Reston, Va.

Sand-Jensen, K. (1998), Influence of submerged macrophytes on sediment composition and near-bed flow in lowland streams, *Freshw. Biol.*, *39*(4), 663–679.

Schumer, R., D. A. Benson, M. M. Meerschaert, and B. Baeumer (2003), Fractal mobile/immobile solute transport, *Water Resour. Res.*, *39*(10), 1296, doi:10.1029/2003WR002141.

Simon, K. S., C. R. Townsend, B. J. F. Biggs, and W. B. Bowden (2005), Temporal variation of N and P uptake in 2 New Zealand streams, *J. North Am. Benthol. Soc.*, *24*(1), 1–18, doi:10.1899/0887-3593(2005)024<0001:TVONAP>2.0.CO;2.

Stanley, E. H., S. G. Fisher, and N. B. Grimm (1997), Ecosystem expansion and contraction in streams, *BioScience*, *47*(7), 427–435, doi:10.2307/1313058.

Stonedahl, S. H., J. W. Harvey, J. Detty, A. Aubeneau, and A. I. Packman (2012), Physical controls and predictability of stream hyporheic flow evaluated with a multiscale model, *Water Resour. Res.*, *48*, W10513, doi:10.1029/2011WR011582.

Stubbington, R., A. J. Boulton, S. Little, and P. J. Wood (2015), Changes in invertebrate assemblage composition in benthic and hyporheic zones during a severe supraseasonal drought, *Freshw. Sci.*, *34*(1), 344–354, doi:10.1086/679467.

Thomas, S. A., H. Maurice Valett, J. R. Webster, and P. J. Mulholland (2003), A regression approach to estimating reactive solute uptake in advective and transient storage zones of stream ecosystems, *Adv. Water Resour.*, *26*(9), 965–976, doi:10.1016/S0309-1708(03)00083-6.

Valett, H. M., J. A. Morrice, C. N. Dahm, and M. E. Campana (1996), Parent lithology, surface-groundwater exchange, and nitrate retention in headwater streams, *Limnol. Oceanogr.*, *41*(2), 333–345.

von Schiller, D., V. Acuña, D. Graeber, E. Martí, M. Ribot, S. Sabater, X. Timoner, and K. Tockner (2011), Contraction, fragmentation and expansion dynamics determine nutrient availability in a Mediterranean forest stream, *Aquat. Sci.*, *73*(4), 485–497, doi:10.1007/s00027-011-0195-6.

von Schiller, D., D. Graeber, M. Ribot, X. Timoner, V. Acuña, E. Martí, S. Sabater, and K. Tockner (2015), Hydrological transitions drive dissolved organic matter quantity and composition in a temporary Mediterranean stream, *Biogeochemistry*, *123*(3), 429–446, doi:10.1007/s10533-015-0077-4.

Ward, A. S., R. A. Payn, M. N. Gooseff, B. L. McGlynn, K. E. Bencala, C. A. Kelleher, S. M. Wondzell, and T. Wagener (2013), Variations in surface water-ground water interactions along a headwater mountain stream: Comparisons between transient storage and water balance analyses, *Water Resour. Res.*, *49*, 3359–3374, doi:10.1002/wrcr.20148.

Warfe, D. M., and L. A. Barmuta (2006), Habitat structural complexity mediates food web dynamics in a freshwater macrophyte community, *Oecologia*, *150*(1), 141–154, doi:10.1007/s00442-006-0505-1.

Watts, G., et al. (2015), Climate change and water in the UK—Past changes and future prospects, *Prog. Phys. Geogr.*, *39*(1), 6–28, doi:10.1177/0309133314542957.

Webster, J. R., et al. (2003), Factors affecting ammonium uptake in streams—An inter-biome perspective, *Freshw. Biol.*, *48*(8), 1329–1352, doi:10.1046/j.1365-2427.2003.01094.x.

Westwood, C. G., R. M. Teeuw, P. M. Wade, N. T. H. Holmes, and P. Guyard (2006), Influences of environmental conditions on macrophyte communities in drought-affected headwater streams, *River Res. Appl.*, *22*(6), 703–726, doi:10.1002/rra.934.

Wilby, R. L., L. E. Cranston, and E. J. Darby (1998), Factors governing macrophyte status in Hampshire chalk streams: Implications for catchment management, *Water Environ. J.*, *12*(3), 179–187, doi:10.1111/j.1747-6593.1998.tb00170.x.

Wilby, R. L., et al. (2010), Evidence needed to manage freshwater ecosystems in a changing climate: Turning adaptation principles into practice, *Sci. Total Environ.*, *408*(19), 4150–4164, doi:10.1016/j.scitotenv.2010.05.014.

Wilcock, R. J., P. D. Champion, J. W. Nagels, and G. F. Croker (1999), The influence of aquatic macrophytes on the hydraulic and physico-chemical properties of a New Zealand lowland stream, *Hydrobiologia*, *416*(0), 203–214, doi:10.1023/A:1003837231848.

Wright, J. F., and A. D. Berrie (1987), Ecological effects of groundwater pumping and a natural drought on the upper reaches of a chalk stream, *Regul. Rivers Res. Manag.*, *1*(2), 145–160, doi:10.1002/rrr.3450010205.

Young, R. G., and A. D. Huryn (1996), Interannual variation in discharge controls ecosystem metabolism along a grassland river continuum, *Can. J. Fish. Aquat. Sci.*, *53*(10), 2199–2211.

Zar, J. H. (2010), *Biostatistical Analysis*, 5th ed., Prentice-Hall, Inc., Upper Saddle River, NJ.

Zarnetske, J. P., R. Haggerty, S. M. Wondzell, and M. A. Baker (2011), Labile dissolved organic carbon supply limits hyporheic denitrification, *J. Geophys. Res.*, *116*, G04036, doi:10.1029/2011JG001730.